Title

A permeabilized cell model for studying cell division: a comparison of anaphase chromosome movement and cleavage furrow constriction in lysed PtK1 cells.

Journal

Journal of Cell Biology, 88(3)

ISSN

0021-9525

Authors

Cande, WZ
McDonald, K
Meeusen, RL

Publication Date

1981-03-01

DOI

10.1083/jcb.88.3.618

Peer reviewed

A Permeabilized Cell Model for Studying Cell Division: A Comparison of Anaphase Chromosome Movement and Cleavage Furrow Constriction in Lysed PtK_1 Cells

W. ZACHEUS CANDE, KENT McDONALD, and RONALD L. MEEUSEN
Department of Botany, University of California, Berkeley, California 94720. Dr. Meeusen's present address is Rohm and Haas, Springhouse, Pennsylvania 19477.

ABSTRACT After lysis in a Brij 58-polyethylene glycol medium, PtK_1 cells are permeable to small molecules, such as erythrosin B, and to proteins, such as rhodamine-labeled FAB, myosin subfragment-1, and tubulin. Holes are present in the plasma membrane, and the mitochondria are swollen and distorted, but other membrane-bounded organelles of the lysed cell model are not noticeably altered. After lysis, the mitotic apparatus is functional; chromosomes move poleward and the spindle elongates. Cells lysed while in cytokinesis will continue to divide for several minutes. Addition of crude tubulin extracts, MAP-free tubulin, or taxol to the lysis medium retards anaphase chromosome movements but does not affect cleavage. On the other hand, *N*-ethylmaleimide-modified myosin subfragment-1, phalloidin, and cytochalasin B inhibit cleavage but have no effect on anaphase chromosome movements under identical lysis conditions. These results suggest that actomyosin plays no functional role in anaphase chromosome movement in mammalian tissue culture cells and that microtubule depolymerization is a rate-limiting step for chromosome-to-pole movements.

In animal cells, two special organelles are formed at the time of division to effect the mechanical separation of cellular and nuclear components. During prophase, the mitotic apparatus forms and subsequently generates the forces that separate chromosomes. During telophase, a contractile ring of microfilaments is organized in the peripheral cytoplasm and it produces the cleavage furrow that divides the cytoplasm in two. Although the organization of the cleavage furrow is not well understood, the mechanochemistry of this process is thought to be similar to muscle contraction and involves the interaction of actin microfilaments and myosin in the contractile ring to constrict the cortex of the dividing cell (4, 38).

The mechanism of anaphase chromosome movement is not well understood (11, 29–31). It has long been recognized that anaphase consists of two distinct motile events; movement of chromosomes to the spindle poles and pole-from-pole separation. These stages of anaphase may represent two physiological events. Structural studies of the rearrangement and redistribution of microtubules at anaphase suggest that each motile event may be associated with a particular class of microtubules (11, 20, 29, 30). Chromosome movement to the poles is associated with kinetochore microtubules and requires kinetochore microtubule depolymerization. Spindle elongation is associated with a redistribution and change in length of nonkinetochore microtubules. At present, the literature favors three classes of theoretical models to explain how chromosomes move. In one class of models, forces necessary to move chromosomes are generated by changing the lengths of the spindle microtubules (9, 20, 29, 30). Alternatively, forces are generated by dynein like cross-bridges and sliding microtubules (7, 21, 24, 25, 29, 30, 32) or by an actomyosin system interacting with a microtubule scaffold (5, 10, 12, 34).

To understand and dissect the mechanism of anaphase chromosome movement, we have developed a method of cell permeabilization that is compatible with the maintenance of chromosome movement after lysis (2–7). Controlled mild lysis of dividing PtK_1 cells is obtained by manipulating the levels of nonionic detergent and polyethylene glycol in the lysis medium (2). In the Appendix, we describe the ultrastructure and permeability properties of the lysed cell models. We have used lysed

THE JOURNAL OF CELL BIOLOGY · VOLUME 88 MARCH 1981 618-629

cells models to demonstrate an ATP requirement for anaphase chromosome movement and a vanadate inhibition for this process (3, 7). Recently, we have shown that permeabilized dividing cells will also undergo cleavage (4), and in this paper we compare the sensitivity of cleavage and anaphase chromosome movement with various classes of inhibitors.

Using the permeabilized cell models we address two fundamental problems of spindle mechanochemistry; what are the relative roles of microtubule polymerization-depolymerization and of actomyosin during anaphase? The permeabilization procedure allows us to introduce into cells proteins, such as tubulin and NEM-S_1 (*N*-ethylmaleimide-modified myosin subfragment-1), and drugs, such as taxol and phalloidin, that normally enter the cell slowly or not at all. Because the lysis procedure is compatible with both cleavage and anaphase chromosome movement, we are able to compare directly the effects of these treatments on a process of known mechanochemistry, i.e., cleavage, with that of unknown mechanochemistry, i.e., chromosome movement.

MATERIALS AND METHODS

Materials

Vanadate-free ATP prepared from yeast was obtained from Boehringer-Mannheim Biochemicals, Indianapolis, Ind. Carbowax 20 M (polyethylene glycol, 20,000 mol wt), cytochalasin B, and Brij 58 were obtained from Sigma Chemical Co., St. Louis, Mo. and erythrosin B (5′, 7′ tetraiodofluoroscein, 890 mol wt) was obtained from Eastman Organic Chemicals, Rochester, N. Y. Phalloidin was a gift from T. Wieland (Max Planck Institute für Chemie, Heidelberg) and taxol was a gift from John Douros (National Cancer Institute, Bethesda, Md.). Stock solutions of taxol and cytochalasin B were made up in dimethyl sulfoxide (DMSO) and these drugs were added such that the final concentration of DMSO in the lysis medium was 1%.

Myosin subfragment-1 (S_1) was prepared from rabbit skeletal myosin by the method of Weeds and Taylor (42). NEM-S_1 and NEM-modified bovine serum albumin (NEM-BSA) were prepared as described previously (4, 26).

A new procedure was used to prepare fluorescein-labeled S_1 that will be described in more detail later (Cande, manuscript in preparation). 10 mg/ml S_1 was incubated with 1 mM fluorescein-5-maleimide (Molecular Probes, Roseville, Minn.) for 30 min at room temperature in 10 mM imidazole-Cl, pH 7.0, 0.2 mM dithiothreitol. The reaction was stopped by the addition of 10 mM dithiothreitol. The S_1 was precipitated by the addition of saturated NH_4SO_4 to 60%. It was pelleted by centrifugation. The pellet was resuspended in incubation buffer and run over a Biogel P-2 column (Bio-Rad Laboratories, Richmond, Calif.) and the void volume was collected. This procedure was repeated and the sample was then dialyzed several days against the same buffer. After centrifugation to clarify the solution, the yield of fluorescein-labeled protein was 10–15% of the starting material. As determined spectrophotometrically by measuring absorbance at 495 nm, there was 0.8–1.0 fluorescein/S_1 molecule. The ATPase activity of this preparation was measured as previously described (26) and was similar to the unlabeled S_1. This preparation stained the I bands of glycerinated myofibrils.

Beef neurotubulin was prepared by two cycles of polymerization and depolymerization and was stored frozen until the day of use (39). The protein was resuspended in 100 mM PIPES, pH 6.9, 1 mM $MgSO_4$, 1 mM EGTA, and 1 mM GTP, and then added at the appropriate dilution to the lysis medium. MAP-free tubulin was prepared by phosphocellulose chromatography as previously described (44), with the modification that 100 mM Pipes, 1 mM $MgSO_4$, 1 mM EGTA was used as the buffer solution. SDS polyacrylamide gel electrophoresis was run as previously described (39).

Precise levels of free calcium in the lysis medium were maintained with a Ca/EGTA buffering system, designed to compensate for the presence of 1-mM excess Mg^{++} and Mg ATP at a defined pH (4).

Tissue Culture Cells and Cell Lysis

PtK_1 cells were used in all experiments and were maintained and handled for light microscopy as previously described (39). Cover slips were mounted on slides with cover slip fragments as spacers. Cells engaged in cell division were lysed by flushing solutions under the cover slip in a two-step lysis procedure. Step A medium contained 85 mM PIPES, 0.08–0.1% Brij 58, Ca/EGTA buffers, 1.25 mM ATP, 2.25 mM $MgSO_4$. Step B, which followed 70–90 s after step A, used a similar medium that included in addition 2.5% polyethylene glycol (Carbowax 20 M) and 0.1–0.15% Brij 58. For studying anaphase chromosome movement, cells were lysed into solutions containing 1 mM EGTA or 0.1 μM free calcium. In some cleavage experiments, cleavage was delayed 70–90 s by increasing the free calcium levels to 4 μM and removing Mg ATP (4). Cleavage was then reinitiated by lowering the calcium levels to 0.1 μM and adding Mg ATP to step B (4).

In the dye penetration studies, cells were flushed with tissue culture medium or lysis medium containing 0.5% erythrosin B. In some experiments, dye was not added until 1 min before the rinse step. At the end of the experiment, cells were rinsed with several changes of solution B without dye, and the cells were then photographed with bright field optics and a green wide band pass 540 nm interference filter (Orion Research, Inc., Boston, Mass.).

For studying fluorescent-S_1 and rhodamine-labeled FAB uptake (papain digested goat anti-rabbit immunoglobulin fraction, 50,000 mol wt, three rhodamines/FAB, a gift from Leon Wolfsy), 0.5–3 mg/ml of protein was included in the lysis medium. At the end of the incubation period, cells were flushed for 1 min with step B medium without the protein, and then fixed in 3.7% formaldehyde in 100 mM PIPES, pH 6.9, 5 mM $MgSO_4$, 5 mM EGTA. The cells were mounted in 20% glycerol, 50 mM EPPS (4-[2-hydroxethyl]-1-piperazine propane sulfonic acid), pH 8.0, 5 mM $MgSO_4$, and examined with a Zeiss epifluorescence microscope equipped with phase optics as previously described (5).

The chambers held ~40 μl of lysis medium. At each step, 200 μl (five × volume) of medium were flushed through the chamber during a 20-s exchange period using bibulous paper to facilitate flow. All experiments were run at 35 ± 2°C.

Light Microscopy

Films of dividing cells were made with Zeiss Nomarski or phase optics and an Opti Quip (Opti Quip Inc., Highland Mills, N. Y.) 16-mm cine time-lapse apparatus. Exposures of 1.0-s duration were made at a rate of 10 frames/min. Rates of movement were estimated by measuring the slopes of the graphs drawn of chromosome-chromosome and pole-pole distances from the moment of addition of the second step medium to the position of maximum displacement of chromosomes or poles. The rate of chromosome-to-pole movement was calculated as one-half the difference between the rates of chromosome separation and spindle elongation. Measurements of spindle birefringence were made with a Zeiss polarization microscope equipped with a Brace-Kohler λ/30 compensator (39).

Electron Microscopy

Cells up to 8 min after lysis were monitored by light microscopy to assure that chromosome movement continued, and were then fixed by flushing 1% glutaraldehyde in 0.1 M PIPES at pH 6.94, 2.5 mM Mg^{++} at 37°C under the cover slip. The position of the cell on the cover slip was marked with a diamond-tipped scribe mounted on the objective lens turret. The cover slip was then transferred to a dish of fixative for 30 min. Cells were rinsed in the buffer + Mg^{++} at 37°C (three rinses of 5 min each), transferred to 0.2% tannic acid (Mallinckrodt Inc., St. Louis, Mo.; AR 1764) in buffer + Mg^{++} for 30 min at 37°C, rinsed as above, and then put into 1% OsO_4 in buffer at 4°C for 30 min. Cells were rinsed in distilled H_2O (room temperature) and put in 1% aqueous uranyl acetate at room temperature for 30 min. An acetone series was used for dehydration and the cells embedded in Epon-Araldite by inverting the coverslip over a small plastic cap (18-mm diameter) filled with resin. After polymerization of the resin, the position of the marked cell was noted and the cover slip was removed from the resin wafer by immersion in liquid nitrogen. The cell was cut from the resin wafer and remounted such that sections through it would be perpendicular to the flattened bottom surface of the cell. Silver sections were cut on a Porter-Blum MT-2B microtome (DuPont Instruments, Wilmington, Del.), poststained with lead nitrate and uranyl acetate, and viewed in a JEOL 100s electron microscope at 80 keV.

RESULTS

Tubulin Inhibition of Chromosome Movement

During the first 10–12 min after lysis, both chromosome-to-pole movements and spindle elongation continue in permeabilized anaphase cells (Fig. 1 *a–d*) at rates ~50% that observed in vivo. Although the rates observed may vary over time, the rate and extent of movement in any one experimental series is usually consistent and reproducible. As previously described, chromosome movement requires Mg (3) and ATP (3, 7), and is reversibly inhibited by vanadate in the V^+ oxidation state (7).

Addition of polymerizable neurotubulin to the lysis medium retards chromosome-to-pole movements and spindle elongation (Figs. 1 and 2 and Table I). Tubulin prepared by two cycles of polymerization and depolymerization (2× tubulin, Fig. 1 *i*) is ~80% tubulin- and 20% microtubule-associated proteins (MAPs) and will self-assemble into microtubules in the lysis medium. After lysis in 4 mg/ml 2× tubulin, anaphase continues but the chromosomes do not reach the spindle poles (Figs. 1 *e–h* and 2 *b*). In the examples selected, although the chromosomes move several micrometers after lysis, at the end of the experiment they are still 2–3 μm from the poles. In control experiments run at the same time, chromosomes move farther and more closely approach the spindle poles (Figs. 1 *a–d* and 2 *a*). Rates of chromosome separation, spindle elongation, and chromosome-to-pole movements are inhibited by at least 50% compared with cells lysed in BSA or polymerization incompetent tubulin prepared by repeated freezing and thawing over several days (Table I).

MAP-free tubulin (Fig. 1 *i*) does not self-assemble in the lysis medium but is capable of self assembly upon addition of MAPs. Lysis in MAP-free tubulin also retards anaphase chromosome movements, although not to the same extent as lysis in 2× tubulin, and preferentially inhibits chromosome-to-pole movements (Fig. 2 *c* and Table I). Rates of spindle elongation are inhibited by ~25% in 1–2 mg/ml MAP-free tubulin but chromosome-to-pole movements are inhibited by at least 50%.

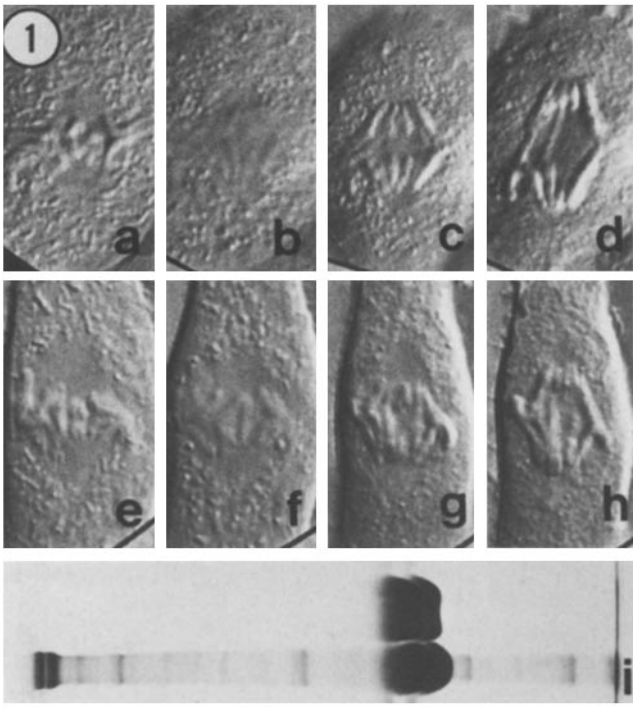

FIGURE 1 Effect of tubulin on chromosome separation in permeabilized PtK_1 cells. Cine record of cells lysed without (*a–d*) or with (*e–h*) 4 mg/ml tubulin. *a* and *e*, Before lysis; *b* and *f*, 1 min after lysis; *c* and *g*, 3 min after lysis; and *d* and *h*, 8 min after addition of lysis medium. × 1,900. (*i*) SDS polyacrylamide gel of MAP-free tubulin (upper line) and crude tubulin preparation (lower line).

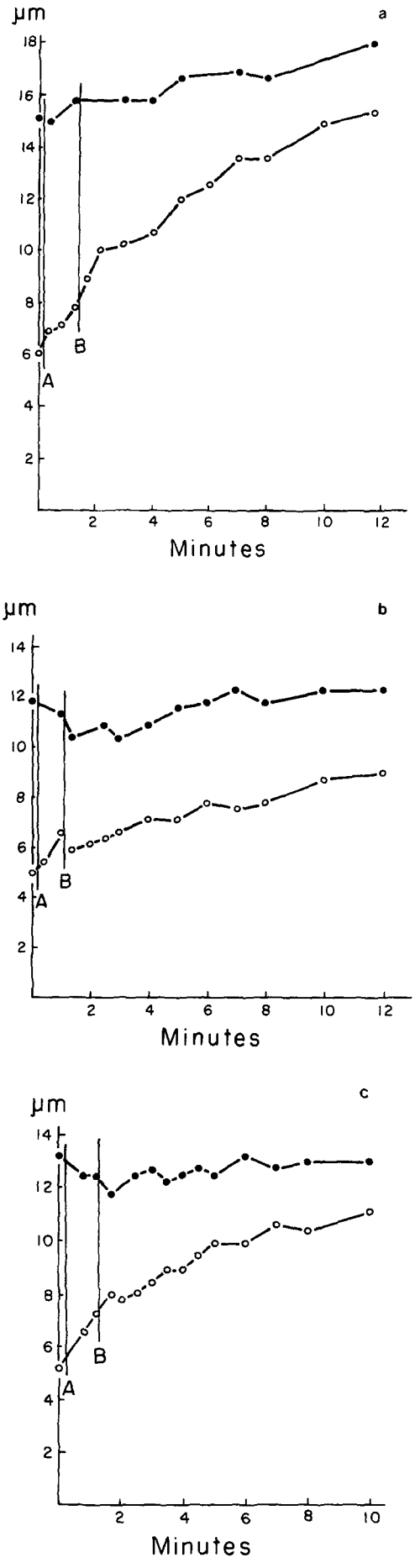

FIGURE 2 Effect of tubulin on chromosome separation in permeabilized PtK_1 cells. In *a–c*, separation of spindle poles (filled circles) and sister chromatids (open circles) after lysis. *a*, Lysis medium containing 4 mg/ml BSA; *b*, 4 mg/ml 2× tubulin; *c*, ~1 mg/ml MAP-free tubulin.

TABLE I

Effect of Tubulin on Chromosome Movements

Treatment	No. of experiments	Rates of movement: Chromosome separation	Spindle elongation	Chromosome-to-pole movement
			μm/min	
Series A				
BSA, *4 mg/ml*	4	0.94 ± 0.13*	0.60 ± 0.29	0.18 ± 0.09
Denatured tubulin, *4 mg/ml*	2	0.99	0.64	0.18
Tubulin, *4–5 mg/ml*	6	0.44 ± 0.20	0.29 ± 0.19	0.07 ± 0.10
Series B				
No protein	5	0.84 ± 0.07	0.39 ± 0.10	0.23 ± 0.04
MAP-free tubulin, *1–2 mg/ml*	9	0.51 ± 0.04	0.29 ± 0.04	0.11 ± 0.03

* Standard deviation.

Taxol Inhibition of Chromosome Movement

Taxol, an experimental antitumor agent, has been demonstrated to promote microtubule assembly in vitro and stabilize microtubules against depolymerization by cold and calcium in vitro and in vivo (36). Lysis in 2 μM taxol blocks all chromosomal movements and spindle elongation, but at lower concentrations taxol preferentially retards chromosome-to-pole movement (Table II). In some experiments (Fig. 3 *a–d*), chromosomes and poles move together after lysis as the spindle elongates and the chromosomes do not approach the poles.

When added to the culture medium at the beginning of anaphase, 100 μM taxol freezes the spindle and retards further chromosome movements (Fig. 3 *e–p*). The spindle persists unnaturally into telophase and continues to exclude the rod-shaped mitochondria from around the chromosomes and in the spindle midzone. Even though the spindle remains as a birefringent organelle (Fig. 3 *m–p*), the chromosomes begin to decondense. During cytokinesis, the spindle is then deformed as the cleavage furrow attempts to pinch the cell in two. At this time, a large spindle remnant is still present around the spindle poles and the spindle midbody is extraordinarily large (Fig. 3 *o–p*). Because the spindle persists as a birefringent body, although it is deformable by the cytokinetic furrow, the effect of taxol to inhibit anaphase chromosome movements must not be caused by spindle dissolution.

Inhibitors of Actomyosin-based Motility Do Not Inhibit Anaphase

As previously described (4, 26, 27), NEM-HMM and NEM-S_1 bind to actin in a rigorlike bond even in the presence of MgATP. Preincubation with 1–2 mg/ml NEM-S_1 blocks glycerinated myofibril contraction, the contraction of cytoplasmic strands of *Chaos* cytoplasm (26), and cleavage in permeabilized PtK_1 cells (reference 4 and Table V) and microinjected amphibian eggs (27).

Addition of NEM-S_1, NEM-BSA, or S_1 has no effect on anaphase chromosome movement (Fig. 4, Table III), although in the same series of experiments, tubulin added at similar concentrations retards chromosome movement by 40–50%. In contrast, the largest differences between NEM-S_1 and any control is ~15%. These differences probably reflect day-to-day

TABLE II

Effect of Taxol on Chromosome Movements

Treatment (drug concentration)	No. of experiments	Rates of movement: Chromosome separation	Spindle elongation	Chromosome-to-pole movement
			μm/min	
None, *1% DMSO*	6	0.64 ± 0.12*	0.21 ± 0.06	0.22 ± 0.06
0.75 μM	5	0.29 ± 0.07	0.23 ± 0.15	0.03 ± 0.06
2.0 μM	4	0.10 ± 0.08	0.0 ± 0.04	0.04 ± 0.04

* Standard deviation.

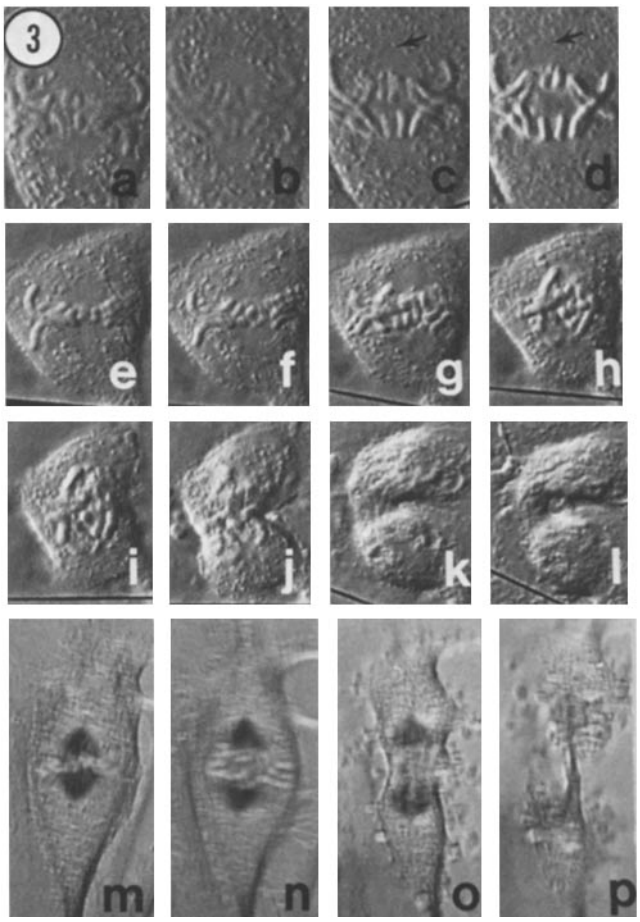

FIGURE 3 Effect of taxol on chromosome movements and cleavage in lysed (*a–d*) and unlysed (*e–p*) PtK_1 cells. a, 0.1 min before lysis; *b*, 2 min after lysis in 0.75 μM taxol; *c*, 4 min after lysis, *d*, 9 min after lysis. × 1,300. Chromosomes do not approach poles (arrows). In the next series of micrographs (*e–l*), taxol (final concentration, 100 μM) was added to the culture medium at the beginning of anaphase. *e*, Just before addition; *f*, after 1 min; *g*, 6 min after, *h*, 11 min after; *i*, 15 min after; *j*, 21 min after; *k*, 33 min after and; *l*, 46 min after in medium containing taxol. Although chromosome movements are inhibited, cleavage continues and a large spindle remnant is present in late telophase cell (*j–k*). × 900. Polarization micrographs of unlysed cell just before taxol addition (*m*), after 4 min (*n*), after 12 min (*o*), and after 21 min (*p*) in 100 μM taxol. Note large spindle remnant in *o* and *p*. × 900.

variability in rates of movement. These experiments were repeated using a severalfold higher concentration of NEM-S_1 with similar results (Table III, Series B). Fortuitously, in one experiment, a cleaving cell was located at the edge of the microscope field (Fig. 5). Unlike the anaphase cell, which displayed chromosome movements for 10 min after lysis, the cleaving cell did not continue to divide. Instead, after 1–2 min in the NEM-S_1 medium the furrow stopped contracting and relaxed slightly.

Addition of high concentrations of cytochalasin B (15 μg/ml) and phalloidin (200 μg/ml) to the lysis medium had no effect on chromosome-to-pole movement and spindle elongation (Table IV). In the same series of experiments, under identical lysis conditions, vanadate (7) and taxol blocked chromosome movements.

TABLE III

Effect of NEM-S_1 on Chromosome Movements

Treatment (protein)	No. of experiments	Rates of movement: Chromosome separation	Spindle elongation	Chromosome-to-pole movement
			μm/min	
Series A*				
None	6	0.66 ± 0.14‡	0.25 ± 0.06	0.21 ± 0.07
NEM-S_1, *2 mg/ml*	10	0.65 ± 0.13	0.30 ± 0.16	0.17 ± 0.04
NEM-BSA, *2 mg/ml*	4	0.58 ± 0.12	0.22 ± 0.13	0.22 ± 0.05
S_1, *2 mg/ml*	3	0.76 ± 0.10	0.34 ± 0.06	0.19 ± 0.09
Tubulin, *5 mg/ml*	6	0.36 ± 0.10	0.14 ± 0.11	0.11 ± 0.08
Same day	5	0.73 ± 0.12	0.29 ± 0.10	0.22 ± 0.06
Series B				
NEM-S_1, *7 mg/ml*	3	0.68 ± 0.13	0.35 ± 0.08	0.16 ± 0.04
NEM-BSA, *7 mg/ml*	3	0.73 ± 0.11	0.33 ± 0.06	0.20 ± 0.03

* The results from this series of experiments were compiled from the same 2 wk period. To give some idea of the variations in rates of movement that occurred during one day, we have averaged together the results of one day's experiments regardless of treatment (NEM-S_1, S_1, or none).

‡ Standard deviation.

Inhibitors of Actomyosin-based Motility Inhibit Cleavage

PtK_1 cells lysed during cytokinesis in Brij 58-Carbowax medium continue to undergo cleavage for 5–10 min provided two criteria are met: (*a*) the cell must show visible signs of cleavage furrow formation and function, and (*b*) the free calcium levels in the lysis medium must be below 1 μM (4). An example of the extent of cleavage furrow constriction after lysis is shown in Fig. 7*g–h*. By manipulating the free calcium and MgATP concentrations in the lysis medium it is possible to stop and restart cleavage. Cleavage can be stopped for several min by raising the free calcium concentration to 4 μM in the absence of MgATP and can be reinitiated by lowering the calcium level to 0.1 μM in the presence of MgATP. We have used this protocol to study the effects of NEM-S_1, cytochalasin

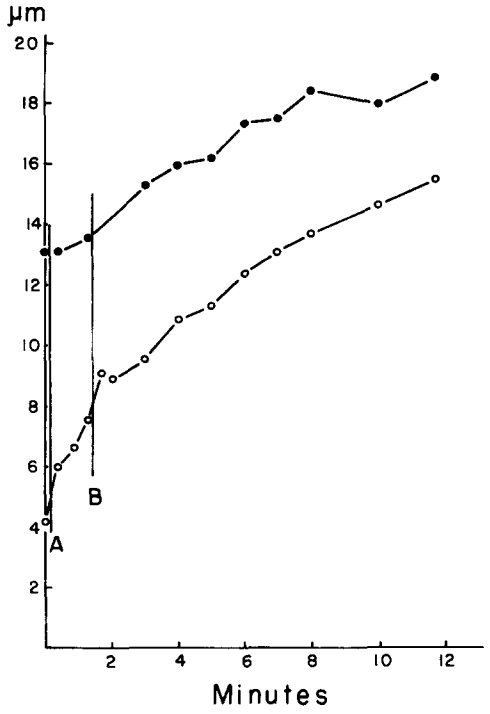

FIGURE 4 Effect of NEM-S_1 on chromosome separation in permeabilized PtK_1 cells. Separation of spindle poles (full circles) and sister chromatids (open circles) after lysis in 7 mg/ml NEM-S_1.

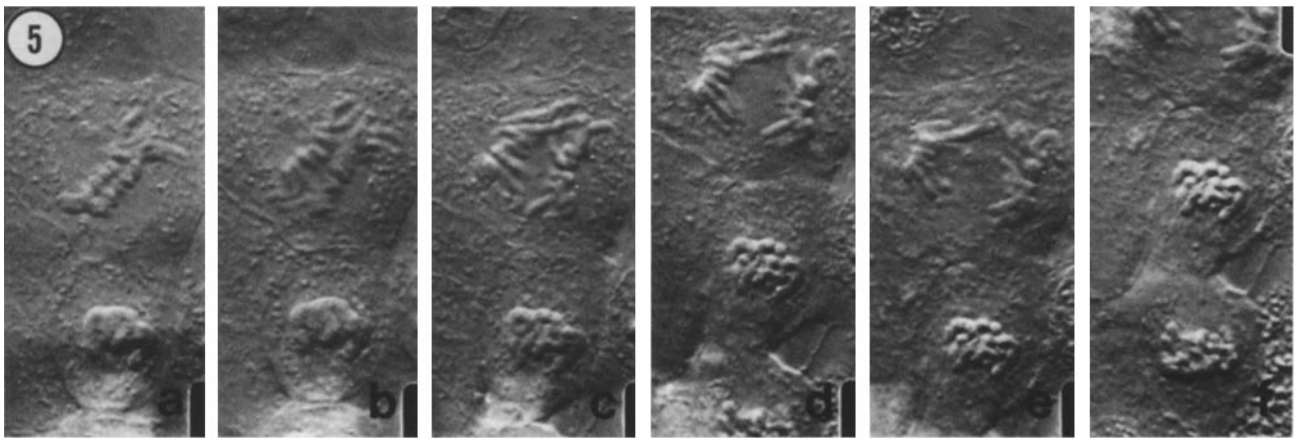

FIGURE 5 Effect of NEM-S_1 on chromosome separation and cleavage in permeabilized PtK_1 cells. *a*, 0.1 min before lysis; *b*, 1 min after lysis in 7 mg/ml NEM-S_1; *c*, 4 min after lysis; *d*, 8 min after lysis; *e*, 12 min after lysis; *f*, adjacent cleaving cell after 12 min in NEM-S_1. In micrographs *a–e*, the top half of the cell undergoing cleavage can be seen in the lower portion of the frame. × 1,600.

B, and phalloidin on cleavage. These experiments are described in detail in another paper (4) and are summarized in Table V. We would like to emphasize that these experiments and the inhibitor studies on anaphase chromosome movement were run during the same period of time and the lysis conditions, with the exception of the free calcium levels in the medium, were identical.

NEM-S_1 blocks cleavage after a 70–90 s incubation, however, NEM-BSA and S_1 have no effect on cleavage. After lysis in 15 μg/ml cytochalasin B, the furrow undergoes a rapid expansion to several times its original width. At lower concentrations of the drug, furrow relaxation is less extensive. After lysis in 200 μg/ml phalloidin, cleavage is blocked and the furrow neither relaxes nor changes shape (Table V).

Inhibitors of Chromosome Movement Do Not Block Cleavage

Vanadate in the V^+ oxidation state is a potent inhibitor of dynein ATPase activity, and under some circumstances, myosin ATPase activity (7, 13). However, vanadate concentrations 100-fold higher than that required to retard anaphase chromosome movement in permeabilized cells (7) have no effect on cleavage (Table VI). Similarly, we find that lysis of cells into concentrations of neurotubulin and taxol sufficient to inhibit chromosome movement has no effect on extent of cleavage (Table VI).

TABLE IV

Effect of Phalloidin and Cytochalasin B on Chromosome Movements

Treatment	No. of experiments	Rates of movement: Chromosome separation	Rates of movement: Spindle elongation	Rates of movement: Chromosome-to-pole movement
			μm/min	
Phalloidin, *200 μg/ml*	5	0.68 ± 0.09*	0.25 ± 0.14	0.21 ± 0.05
Control	4	0.72 ± 0.18	0.28 ± 0.19	0.22 ± 0.06
Cytochalasin B, *15 μg/ml*	6	0.52 ± 0.08	0.18 ± 0.04	0.17 ± 0.04
Control, *1% DMSO*	6	0.58 ± 0.23	0.22 ± 0.13	0.18 ± 0.12

* Standard deviation.

TABLE V

Effect of Actin-Motility Inhibitors on Cleavage

Treatment	No. of experiments	Extent of constriction*
Proteins‡		
NEM-S_1, *2 mg/ml*	5	−0.08 ± 0.15§
NEM-BSA, *2 mg/ml*	6	0.30 ± 0.20
S_1, *2 mg/ml*	5	0.35 ± 0.20
Cytochalasin B		
15 μg/ml	4	−1.63 ± 0.31
0.5 μg/ml	4	−0.35 ± 0.04
0.1 μg/ml	5	0.35 ± 0.14
None, *1% DMSO*	6	0.49 ± 0.12
Phalloidin‡		
200 μg/ml	4	0.08 ± 0.18
None	4	0.42 ± 0.15

* Measured as change in furrow diameter divided by original furrow diameter. Negative values are a measure of furrow relaxation.

‡ In the protein and phalloidin experiments, cleavage was delayed 70–90 s after lysis by manipulating free calcium levels before it was reinitiated (4).

§ Standard deviation.

TABLE VI

Effect of Mitotic Inhibitors on Cleavage

Treatment	No. of experiments	Extent of constriction*
Vanadate, *1 mM*	5	0.31 ± 0.15‡
Control	4	0.30 ± 0.10
Tubulin, *5 mg/ml*	3	0.29 ± 0.10
Control, resuspension buffer	3	0.32 ± 0.09
Taxol, *1 μM*	3	0.51 ± 0.11
Control, *1% DMSO*	3	0.46 ± 0.15

* Measured as change in furrow diameter after lysis divided by the original furrow diameter.

‡ Standard deviation.

DISCUSSION

The Role of Actomyosin during Anaphase

Using immunocytological techniques and heavy meromyosin decoration, actin and myosin have been shown to be minor spindle components localized primarily in fibers running from chromosome to pole (5, 12, 34, 37 and for review see 1, 10, 21). It has not been established whether these components are functional parts of the spindle that contribute to chromosome movement or are cytoplasmic contaminants introduced naturally during spindle formation or by accident during subsequent experimentation and fixation (for a discussion of this controversy see references 1, 10, and 21). Preliminary physiological evidence does not support a role for actomyosin during anaphase. Myosin antibodies injected in dividing marine eggs block cleavage but not mitosis (22, 23). Amphibian eggs microinjected with NEM-HMM or NEM-S_1 have large zones of uncleaved cytoplasm that contain metaphase and anaphase spindles (27). Sakai et al. (32) have demonstrated that chromosome movement in spindle isolates is blocked by dynein antisera but not by myosin antisera.

In this report, we demonstrate that under identical lysis conditions inhibitors of cleavage do not inhibit anaphase chromosome movement. Given our understanding of how these inhibitors function, (cf. reference 4 for a discussion of the interaction of these inhibitors with the cleavage furrow in lysed cells) we can make several statements that define the extent of actomyosin involvement during anaphase.

First, it is unlikely that myosin participates in moving chromosomes. We have previously shown that vanadate, an ATPase inhibitor, retards chromosome movements and alters spindle function (7). Although it has been demonstrated that myosin ATPase activity is sensitive to vanadate under some physiological conditions (13), we find that cleavage in permeabilized cells is insensitive to this inhibitor. In fact, vanadate at concentrations 100 times higher than necessary to retard chromosome movements and 1,000 times higher than necessary to block flagellar beat does not block cleavage (7). Thus, with regard to vanadate sensitivity, the mitotic apparatus is more like a fla-

gellum than a muscle or a cleavage furrow. This observation is consistent with the observed insensitivity of anaphase chromosome movement to NEM-S_1.

NEM-S_1 binds to actin filaments at the myosin binding site and prevents native myosins and other actin binding proteins from interacting at the same site under physiological conditions (4, 28, 29). Although we cannot know with certainty how much NEM-S_1 enters the spindle, lysis in 7 mg/ml NEM-S_1 (5×10^{-5} M) blocks cleavage but not anaphase in the same preparation. These results are consistent with the suggestion that myosin is not mechanochemically involved in chromosome movement.

Second, actin depolymerization is not required for chromosome-to-pole movements. Phalloidin in vitro and in microinjected cells blocks actin depolymerization (8, 43), and in the permeabilized cell model its addition retards cleavage (4). Although the histological and immunofluorescent evidence suggests that actin is primarily associated with the chromosomal fibers in the spindle and the chromosomal fibers shorten during anaphase (5, 12, 34, 37), phalloidin does not interfere with chromosome-to-pole movements in the lysed cell model. This suggests that the actin association with the chromosomal fiber is not a functional one because the fiber must shorten as chromosomes move poleward (11, 20, 29, 30). In contrast, taxol, a drug known to block microtubule depolymerization, preferentially retards chromosome-to-pole movements.

Third, actin gels are not required for chromosome movements. At the high concentrations used in these studies, cytochalasin B solates actin gels in vitro and promotes actin depolymerization (15, 40). In vivo, cytochalasin B blocks cleavage but not chromosome movement (35, 38, 40). After lysis, cytochalasin B has an immediate and dramatic effect to relax the cleavage furrow (4) but has no effect on anaphase chromosome movement. Unless the actin associated with the spindle is protected against cytochalasin B action, actin networks similar to that found in the cytoplasm are not functional parts of the spindle.

The argument has been raised that cytochalasin B does not disrupt mitosis in living cells because the drug may interfere with microfilament organization only by disrupting microfilament-membrane attachment (10, 40). However, it is now recognized that there are extensive membrane systems in the spindle associated with the kinetochore microtubules (11, 16) so that the potential for microfilament-membrane interactions is also present in the mitotic apparatus. Nevertheless, anaphase chromosome movement is cytochalasin B insensitive.

Throughout these studies, we used cleavage as a control in studying the effects of actomyosin inhibitors on chromosome movement in lysed cells. The cleavage system is a reasonable control in that it continues to function after lysis under the same conditions required for maintenance of anaphase chromosome movement in PtK_1 cells. However, cleavage is not a perfect control. One objection is that the contractile ring is located in the cortex of the cell and, after lysis, it should be more accessible to proteins than the spindle, which is buried in the cytoplasm 3–5 μm from the cell surface (cf Fig. 14). In the Appendix, we describe in detail the permeability of lysed cells to proteins. Here we have demonstrated that the spindle is functionally accessible to another protein, tubulin, that has a similar molecular weight to NEM-S_1 (42). Another objection is that the morphology of the contractile ring is fundamentally quite different than that of the spindle. Many microfilaments are present in the contractile ring but few are present in the spindle. Although microtubules are the major fibrous component of the spindle, no microtubules are present in the contractile ring. It has been demonstrated that microfilament-microtubule interactions can occur in vitro mediated by microtubule-associated proteins (14). If such actin-microtubule interactions are essential for spindle function, we are unable to study them during cleavage and we have no way to demonstrate that we can inhibit this type of interaction in the permeabilized cell. We must also recognize that the number of actomyosin interactions that are potentially involved in moving chromosomes may be far fewer than the number involved in cleavage (29, 30, 31, 38). Although these differences between the two systems may have influenced the way inhibitors could interact with the two organelles, we think it more likely that actomyosin is not involved in moving chromosomes.

We suggest that actin and the other muscle-related proteins found in the mammalian mitotic spindle are not functionally important in chromosome movement, but are relocated in the spindle during prophase or during subsequent experimentation. In microinjection experiments, Wang and Taylor (41) have demonstrated that the spindle in sea urchin eggs, because of its unique geometry, can act as a trap or sink for fluorescently labeled proteins in the cytoplasm. A similar process may be going on during prophase with native actin because the cytoskeleton of most interphase cells is disassembled and rearranged during cell division, and a large pool of unpolymerized or poorly organized actin may be present in the cytoplasm of the prophase cell. This actin would then be incorporated passively into the matrix of the spindle but would play no role in chromosome movement.

Role of Microtubule Polymerization-Depolymerization during Anaphase

Inoué (20) has demonstrated that spindle microtubules are in a steady state or "dynamic" equilibrium with a subunit pool of tubulin. Under these conditions, lysis in polymerizable neurotubulin should affect spindle structure and function. As previously described (39), and in the Appendix, lysis in neurotubulin leads to an increase in aster size and overall spindle birefringence, but not to an increase in metaphase spindle length. These results suggest that after permeabilization, the neurotubulin in the medium can be incorporated directly into the spindle, but we cannot rule out the possibility that in these gently lysed cells exogenous neurotubulin also promotes some incorporation of retained native (endogenous) tubulin into the spindle of the permeabilized cell.

During anaphase, the microtubules in the spindle change length. As chromosomes move poleward, kinetochore microtubules shorten and in some cells, as the spindle elongates, the nonkinetochore microtubules increase in length (11, 20, 29, 30). It has been suggested that these length changes in themselves may produce the forces that move chromosomes during anaphase (9, 20, 29, 30). Alternatively, microtubule length changes, particularly microtubule depolymerization, may regulate the rate of chromosome movement (29, 30). Consistent with the hypothesis that kinetochore microtubule depolymerization is a rate-limiting and/or force-generating step, we find that the rate of chromosome-to-pole movement is reduced by the addition of polymerizable tubulin to the lysis medium and that taxol preferentially retards the poleward approach of chromosomes. These results are consistent with in vivo and in vitro studies demonstrating that experimentally induced depolymerization of microtubules can move chromosomes poleward (20, 33).

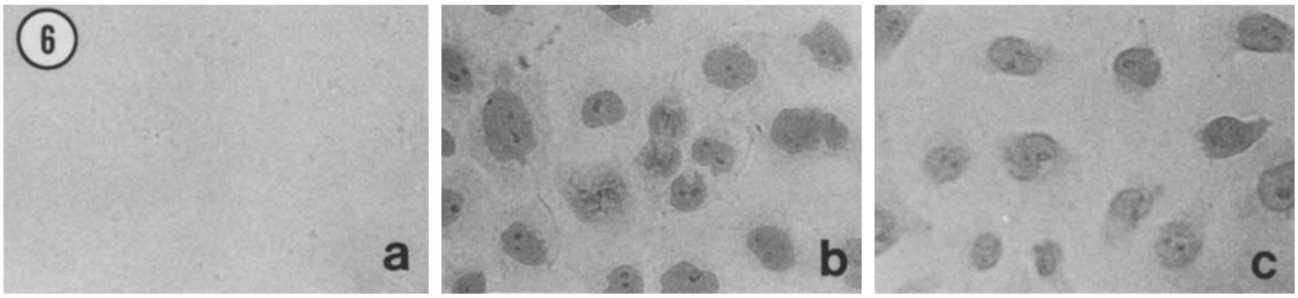

FIGURE 6 Uptake of erythrosin B by PtK_1 cells. *a*, Unlysed cells exposed 4 min to dye; *b*, cells lysed 1 min before addition of dye for 1 min; and *c*, cells lysed 6 min before addition of dye for 1 min. Bright field micrographs. × 650.

However, we are unable to determine from these studies whether microtubule depolymerization is a rate-limiting step or a force-generating requirement for chromosome-to-pole movements.

By addition of tubulin and taxol to the lysis medium, we also directly affect the rate and extent of microtubule growth in the spindle. According to the theoretical models in the literature (9, 20), this treatment should increase the rate and extent of spindle elongation. However, our results are not consistent with that prediction. Crude tubulin extracts and high concentrations of taxol inhibit spindle elongation, and under no circumstances do we actually promote spindle elongation.

We can offer no explanation consistent with any theoretical model of force generation for these results. Inhibition of spindle elongation may be an artifact of new and nonphysiological microtubule growth in the spindle. Extensive aster growth to several times normal size after lysis in tubulin may create increased resistance to spindle movement in the cytoplasm during anaphase. Alternatively, the new microtubules in the spindle may compete with native microtubules for dynein or other microtubule-microtubule interactions necessary for normal spindle elongation. MAPs present in the crude tubulin extract could also compete with spindle "dyneins" for microtubule binding sites (suggested by Joel Rosenbaum, Yale University). To clarify this problem, we plan to study in more detail the effects of tubulin and taxol on spindle elongation by lysing cells late in anaphase after completion of chromosome-to-pole movements. The results of these experiments will be reported at a later date.

APPENDIX

The Permeability Properties and Ultrastructure of Lysed Cell Models

For cell models to be useful in studying cytokinesis and mitosis, the cells after lysis must be permeable to molecules in the bathing solution yet retain lifelike activity. A range of permeabilization procedures has been developed utilizing toluene, lysolecithin, dextran sulfate, etc. (for review see references 17 and 28), however, most of these lysis protocols require conditions that are incompatible with maintaining the structure of the labile mitotic spindle. Glycerol lysis procedures have been used to prepare cytoskeletons and isolated, nonfunctional mitotic spindles, and with the exception of Hoffman-Berling (18, 19), this procedure has not been used successfully to create cell models that undergo chromosome movement and cleavage. The advantage of the lysis protocol described here is that both spindle function and cleavage furrow constriction are maintained after lysis.

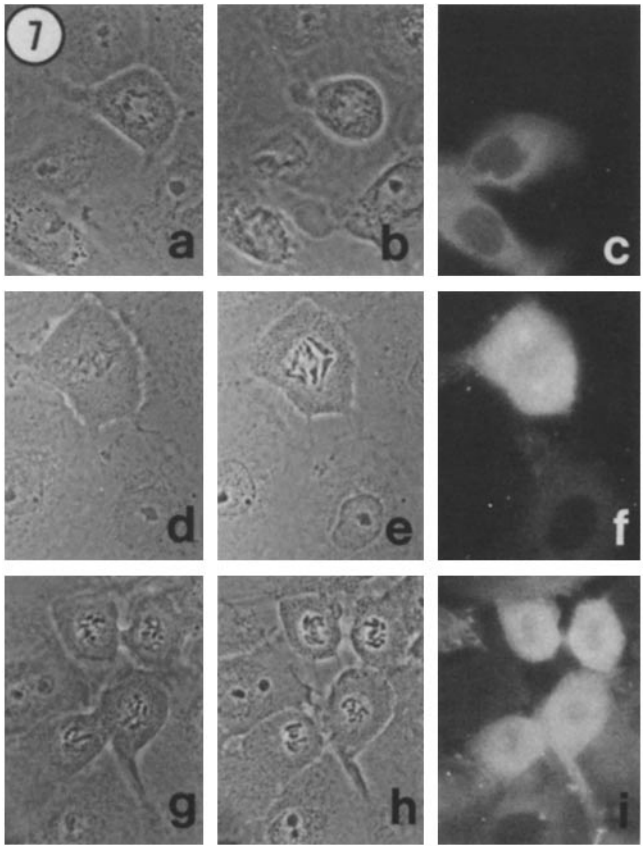

FIGURE 7 Uptake of rhodamine-labeled FAB (1 mg/ml) by lysed PtK_1 cells. Micrographs of dividing cells before lysis (*a*, *d*, and g); after lysis, rinse, and fixation (*b*, e, and *h*); and fluorescent micrographs of the same cells (*c*, *f*, and *i*). In *a*–*c*, the cells were lysed for 1 min before fixation and there was no protein uptake by the anaphase cell. In *d*–*f*, the cells were lysed for 4 min. In *g*–*i*, the cells were lysed for 8 min before fixation. Both cells continued to undergo cleavage after lysis. All observations were made with a Zeiss × 63 Planapo NA 1.4 lens and photographic exposure and development times were similar in all experiments. × 800.

The lysis protocol can be utilized at 37° C and is compatible with reactions like ATP hydrolysis by myosin and microtubule polymerization (Cande, unpublished data). Unlike another protocol we previously described (6), it is not necessary to include tubulin in the lysis medium to maintain spindle structure and function.

After lysis, Ptk_1 cells are permeable to small molecules like erythrosin B (800 mol wt, Fig. 6), and to proteins like rhodamine-labeled FAB (50,000 mol wt), tubulin (110,000 mol

wt), and fluorescein-labeled S_1 (~120,000 mol wt) (2, 3). Erythrosin B uptake by cells occurs only after exposure to detergent and is rapid (Fig. 6). The spindles and chromosomes of dividing cells and the nuclei of interphase cells are stained by the dye even after 1-min exposure to the lysis medium (Fig. 6b). A similar staining pattern is observed when dye is added to the preparation after 7 min in detergent (Fig. 6c), indicating that the permeabilization of the cells is irreversible. In general, all cells in the field are stained by dye.

To monitor the rate and extent of protein uptake, cells were lysed in rhodamine-labeled FAB (50,000 mol wt), then rinsed and fixed at different times after lysis (Table VI, Fig. 7). After 1 min, only a small number of dividing cells on the cover slips were stained (Table VII). After 4 min, most of the dividing cells scored were stained, however, ~14% of the cells were not. Protein penetration was extensive after 8 min because stress fibers in interphase cells (which lie parallel to and near the substrate) were often visible as fluorescently stained structures and 95% of the dividing cells were stained (Table VI). In some experiments, selected cells were monitored from the moment of lysis through the fixation procedure (Fig. 7). After 1 min, most of the interphase cells in the field were stained but the anaphase cell was not (Fig. 7 *a–c*). After 4 min lysis in rhodamine-labeled FAB, the anaphase cell continued to move chromosomes (Fig. 7 *d–f*). The spindle and cytoplasm of this cell were intensely stained. After 8 min in the lysis medium, the cleaving cells in the field of view had undergone further constriction and all of the cells, including the dividing cells, were intensely labeled as a result of protein uptake (Fig. 7 *g–i*). These results demonstrated that permeabilized cells undergoing anaphase chromosome movement or cleavage take up proteins from the lysis medium. However, protein uptake is not as rapid or as uniform as the uptake of smaller molecules like erythrosin B.

We have also documented the uptake of two physiologically important proteins, tubulin and S_1, by permeabilized cells. In this series of experiments, after lysis without tubulin, the metaphase spindle length decreases by 20–30% immediately after addition of lysis medium, and the spindle birefringence fades slowly during the next 10–15 min (Fig. 8 *a* and *c*). After lysis in tubulin, the spindle still shrinks after the first minute in lysis medium, but spindle birefringence

TABLE VII

Rhodamine-labeled Protein Uptake into Permeabilized Cells

Minutes in lysis medium before rinse	No. of dividing cells scored	Stained*		
		Unstained	Weakly stained	Intensely stained
			%	
1	72	57	36	7
4	78	14	27	59
8	74	5	26	69

* For each time point, two cover slips were lysed in a medium containing 0.5–1.0 mg/ml rhodamine-labeled FAB (50,000 mol wt), and after rinsing and fixation were examined with a Zeiss epifluorescence microscope equipped with a ×40 phase Neofluar lens, NA 0.75.

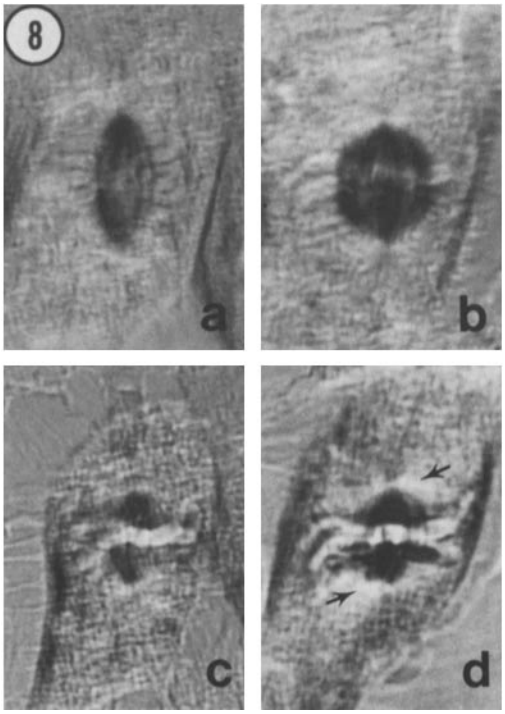

FIGURE 8 PtK_1 cells before and after lysis with or without 4 mg/ml tubulin, as seen with polarization optics. Metaphase cell before lysis (*a*) and 8 min after lysis (*c*) in medium containing 10^{-7} M Ca^{++}. Metaphase cell before (*b*) and 7 min after lysis (*d*) in an identical medium containing in addition 4 mg/ml 2× tubulin. Notice the aster growth in the cell lysed in tubulin (arrows). × 1,700.

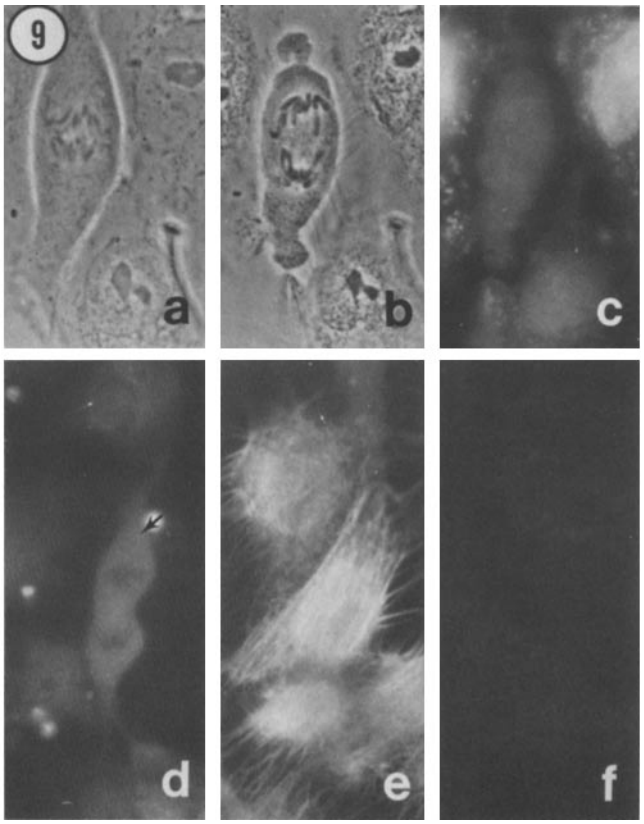

FIGURE 9 Uptake of fluorescein-labeled S_1 by permeabilized PtK_1 cells. Anaphase cell before (*a*) and 5 min after lysis (*b* and *c*) in 3 mg/ml fluorescein-labeled S_1. × 1,100. Field of lysed (*d–e*) and unlysed cells (*f*) after 10 min exposure to 1 mg/ml fluorescein-S_1, rinse and fixation as described in Materials and Methods. Dividing cell indicated by arrow. × 800.

does not fade and persists for hours after lysis (Fig. 8 *b* and *d* and Cande, unpublished data). There is also a noticeable increase in aster birefringence around the spindle poles presumably caused by growth of new polar microtubules in the permeabilized cell (Fig. 8 *d*). No such changes are observed if cells are lysed in aged tubulin incapable of in vitro polymerization.

Fluorescein-S_1 stains almost all the cells on a cover slip after a 5-min lysis period, especially the dividing cells (Fig. 9 *a–e*); however, no staining is observed if the cells are unlysed (Fig. 9 *f*) and staining is decreased if 5 mM ATP is added to the lysis medium. Two types of staining patterns are observed; most cells including all dividing cells are diffusely stained, but in a small number of interphase cells (~5%), the staining is less diffuse and associated primarily with the stress fibers (Fig. 9 *e*). The phase appearance of these interphase cells suggests they are more heavily extracted than the diffusely stained cells. In mitotic cells, there is no increased staining in the spindle but the condensed chromosomes stand out either as regions of increased (Fig.

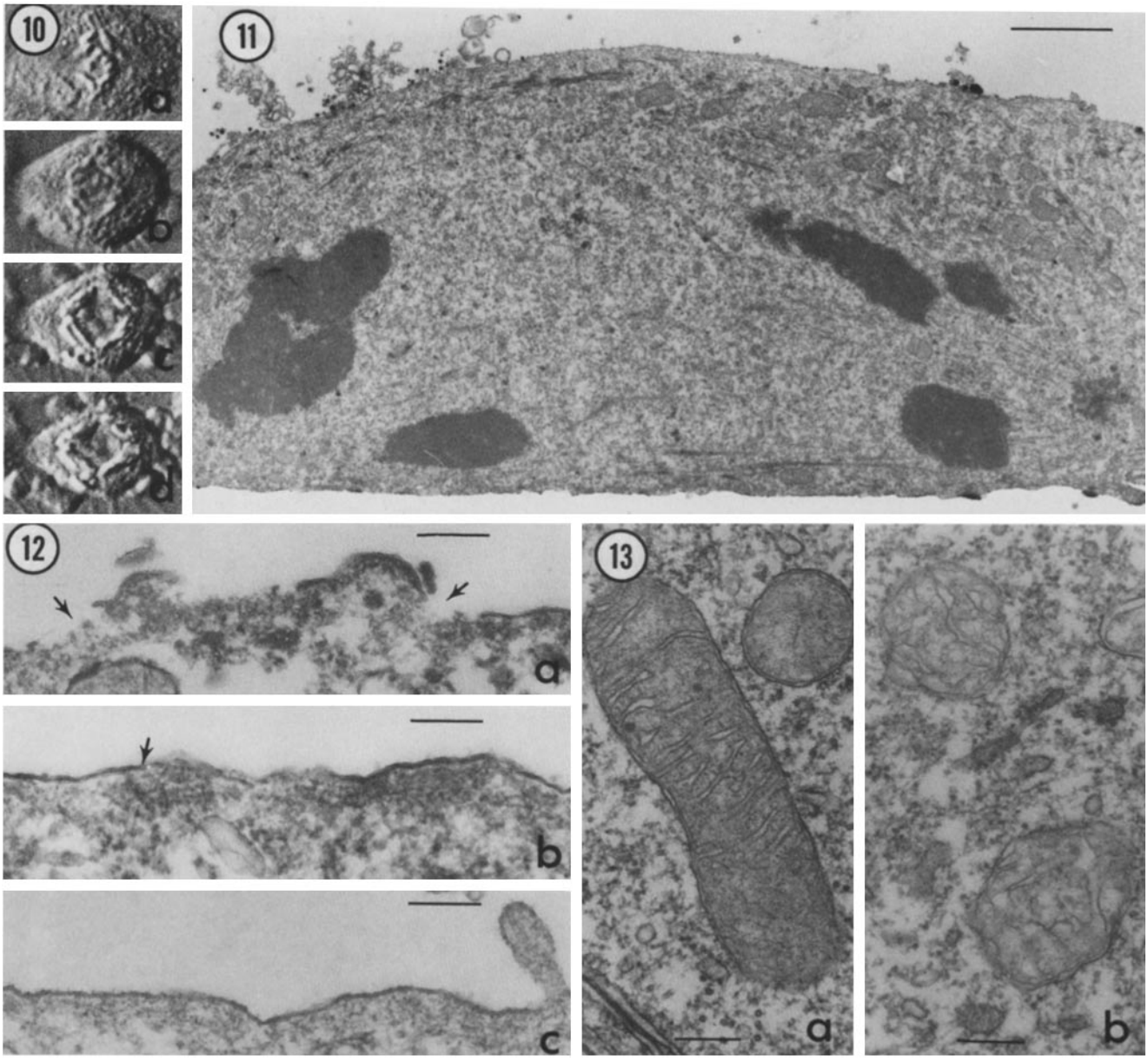

FIGURES 10–13 Ultrastructure of anaphase PtK_1 cells before and after lysis. Fig. 10 shows the cine record of anaphase cell fixed during process of moving chromosomes. *a*, Before lysis; *b*, after 2 min; *c*, after 4 min; and *d*, after 7 min. × 1,200. Fig. 11 shows a longitudinal section of an anaphase spindle cut perpendicular to the substrate on which the cell was growing. At the time of fixation, the cell had been in lysis medium for 8 min and the chromosomes were still moving poleward. Note that the cytoplasm shows little apparent extraction. × 7,500. Bar, 2 μm. Fig. 12 shows the cortex of lysed and unlysed cells. (*a*) Surface of a cell after 8 min in lysis medium. This is the same cell shown in 10 *a–d*. Relatively little plasma membrane (arrow) remains. (*b*) Cell that has retained its plasma membrane (arrow) after 6 min lysis. (*c*) Plasma membrane and cortex of an unlysed dividing cell. × 57,000. Bar, 0.2 μm. Fig. 13 shows the mitochondria of unlysed and lysed cells. (*a*) Mitochondria in an unlysed cell showing typical flattened cristae and elongate shape. (*b*) Mitochondria in a cell after 2 min lysis. The internal membranes appear swollen and the mitochondrial matrix material is less dense than in untreated cells. This round profile is typical; one rarely sees elongate mitochondrial shapes in lysed cells. Bar, 0.2 μm. × 44,000.

9 *c*) or decreased fluorescence (Fig. 9 *d*). In cleaving cells, the cytoplasm is uniformly stained and there is no increase in stain density in the cleavage furrow (Fig. 9 *d*).

We have examined the ultrastructure of cells fixed at various times after lysis (Figs. 10–13). In all cases, the cells examined were known to be moving chromosomes at the time of fixation (Fig. 10 *a–d*). The ultrastructure of these cells is similar but not identical to that of unlysed cells (Fig. 11). The most striking difference is that the plasma membrane of many of the lysed cells was noticeably disrupted. In a few cases, large holes were present in the plasma membrane (Fig. 12 *a*), but some cells did not exhibit a visible change in unit membrane morphology (Fig. 12 *b*). Lysed cells were also characterized by blebs of membrane and other debris attached to their surfaces which were not found on unlysed cells (Fig. 11).

The cytoplasm underneath the disrupted membrane of the lysed cells did not look noticeably different from that of the unlysed cell (Fig. 12 *a–c*). In most cases, the density of staining of the ground substance was similar in both unlysed and lysed cells (cf. Fig. 13 *a* and *b*), and microfilaments, microtubules, and intermediate filaments were found in both classes of cells. Although most cytoplasmic organelles were not disrupted by the lysis protocol, mitochondria in lysed cells were swollen and the cristae distorted (Fig. 13). This change was noticeable even after 2 min in the lysis medium. The mitochondrion shape change was also visible in light micrographs (cf. Fig. 1 *a* and *b*). The changes described above were not progressive. That is, we could find examples of membrane disruption, etc., in cells fixed after 1 or 8 min in the lysis medium and the extent of intracellular disruption did not depend on when the cells were fixed.

Discussion

The mild lysis procedures utilized here produce a cell model with a complexity approaching that of living cells. This complexity may be essential for maintaining spindle and cleavage furrow function and may allow us to eventually manipulate other processes essential to cell division, such as cleavage initiation and spindle formation.

Because the ultrastructure of the lysed cell is similar in background density to that of unlysed cells, we feel confident that our own fixation procedures are giving us a reasonable picture of lysed cell structure. If the cells had appeared to be highly extracted, we would not have known whether these differences reflected the true state of affairs before fixation or were a result of differential susceptibility to extraction during fixation and processing for electron microscopy.

The complexity of the cytoplasm and the presence of membrane-bounded compartments after lysis may provide barriers to uptake and diffusion of molecules throughout the cell model. Although dye uptake is rapid and uniform, fluorescently labeled protein uptake occurs more slowly, and not all cells in a preparation are stained to the same extent by the larger molecules. However, even given these problems of variability, we can demonstrate that NEM-S_1 penetrates the cortex of cells and interacts with the contractile machinery of the cleavage furrow within 90 s after lysis, and that neurotubulin is incorporated into the spindles of permeabilized mitotic cells and interferes with spindle function within several minutes after lysis. In this regard, the unit membrane morphology observed in the plasma membrane and other membrane-bounded organelles may not reflect a functional permeability barrier to dye and protein uptake.

As would be expected, the distribution of fluorescent S_1 in the Brij 58/Carbowax-treated cells was different than the distribution of stain in glycerinated or formaldehyde fixed cells after antiactin or fluorescently labeled heavy meromyosin treatment (12, 15, 21, 34, 37). The majority of interphase cells and all mitotic cells were diffusely stained and in only a few interphase cells were stress fibers predominant. The diffuse image observed in this experiment may be caused by the retention in the permeabilized cell of loosely organized actin, i.e., an actin gel that is lost or rearranged in glycerinated or fixed cells. Alternatively, some of the diffuse staining pattern may be caused by nonspecific trapping of S_1 in the cells even after rinsing.

We would like to thank Susan Stallman for excellent technical assistance and Dr. Greenfield Sludder and Dr. Beth Burnside for helpful discussions.

This study was supported by National Institutes of Health grant GM 23238, Biomedical Research Support grant BRSI 507 RR0706, and American Cancer Society grant CD-79.

Received for publication 19 September 1980, and in revised form 17 November 1980.

REFERENCES

1. Aubin, J. E., K. Weber, and M. Osborn. 1979. Analysis of actin and microfilament-associated proteins in the mitotic spindle and cleavage furrow of PtK_2 cells by immunofluorescence microscopy: a critical note. *Exp. Cell. Res.* 124:93–109.
2. Cande, W. Z. 1978. Chromosome movement in lysed cells. *In* Cell Reproduction. E. Dirksen and D. Prescott, editors. Academic Press, Inc., New York. 457–464.
3. Cande, W. Z. 1979. Anaphase chromosome movement: studies using lysed mitotic cells. *In* Cell Motility: Molecules and Organization. S. Hatano, H. Ishikawa, and H. Sato, editors. University of Tokyo Press, Tokyo. 593–608.
4. Cande, W. Z. 1980. A permeabilized cell model for studying cytokinesis using mammalian tissue culture cells. *J. Cell Biol.* 87:326–335.
5. Cande, W. Z., E. Lazarides, and J. R. McIntosh. 1977. A comparison of the distribution of actin and tubulin in the mammalian mitotic spindle as seen by indirect immunofluorescence. *J. Cell Biol.* 72:552–567.
6. Cande, W. Z., J. Snyder, D. Smith, K. Summers, and J. R. McIntosh. 1974. A functional mitotic spindle prepared from mammalian cells in culture. *Proc. Natl. Acad. Sci. U. S. A.* 71:1559–1563.
7. Cande, W. Z., and S. M. Wolniak. 1978. Chromosome movement in lysed mitotic cells is inhibited by vanadate. *J. Cell Biol.* 79:573–580.
8. Dancker, P., I. Löw, W. Hasselback, and T. Wieland. 1975. Interaction of actin with phalloidin: polymerization and stabilization of F-actin. *Biochim. Biophys. Acta.* 400:407–414.
9. Dietz, R. 1972. Die Assembly-Hypothese der Chromosomenbewegung und die Veränderungen der Spindellange während der Anaphase I in Spermatocyten von *Pales ferruginea*. *Chromosoma (Berl.).* 38:11–76.
10. Forer, A. 1978. Chromosome movements during cell division: possible involvement of actin filaments. *In* Nuclear Division in the Fungi. I. B. Heath, editor. Academic Press, Inc., New York. 21–68.
11. Fuge, H. 1977. Ultrastructure of the mitotic spindle. *Int. Rev. Cytol.* 6:1–58.
12. Fujiwara, K., and T. D. Pollard. 1976. Fluorescent antibody localization of myosin in the cytoplasm, cleavage furrow, and mitotic spindle of human cells. *J. Cell Biol.* 71:848–875.
13. Goodno, C. C. 1979. Inhibition of myosin ATPase by vanadate ion. *Proc. Natl. Acad. Sci. U. S. A.* 76:2620–2624.
14. Griffith, L., and T. D. Pollard. 1978. Evidence for actin filament-microtubule interaction mediated by microtubule-associated proteins. *J. Cell Biol.* 78:958–965.
15. Hartwig, J. H., and T. P. Stossel. 1979. Cytochalasin B and the structure of actin gels. *J. Mol. Biol.* 134:539–553.
16. Hepler, P. K. 1977. Membranes in the mitotic apparatus: their possible role in the control of microtubule assembly. *In* Mechanisms and Control of Cell Division. T. L. Rost and E. M. Gifford, Jr., editors. Dowden, Hutchinson, & Ross, Inc., Stroudsburg, Penn. 212–222.
17. Heppel, L. A., and N. Makin. 1977. Methods of rapidly altering the permeability of mammalian cells. *J. Supramol. Struct.* 6:399–409.
18. Hoffman-Berling, H. 1954. Die glycerinwasserextrahierte Telophasenzelle als Modell der Zytokinese. *Biochim. Biophys. Acta.* 15:332–339.
19. Hoffman-Berling, H. 1954. Die Bedeutung des Adenosintriophosphat für die Zell und Kernteilungsbewegungen in der Anaphase. *Biochim. Biophys. Acta.* 15:226–236.
20. Inoué, S. 1976. Chromosome movement by reversible assembly of microtubules. *Cold Spring Harbor Conf. Cell Proliferation.* 3(Book C):1317–1328.
21. Izutsu, K., K. Owaribe, S. Hatano, K. Ogawa, H. Komada, and H. Mohri. 1979. Immunofluorescent studies on actin and dynein distribution in mitotic cells. *In* Cell Motility: Molecules and Organization. S. Hatano, H. Ishikawa, and H. Sato, editors. University of Tokyo Press, Tokyo. 621–638.
22. Kiehart, D., S. Inoué, and I. Mabuchi. 1977. Evidence that force production in chromosome movement does not involve actomyosin. *J. Cell Biol.* 75:(2, Pt. 2):258 *a* (Abstr.).
23. Mabuchi, I., and M. Okuno. 1977. The effect of myosin antibody on the division of starfish

blastomeres. *J. Cell. Biol.* 74:251–263.
24. Margolis, R. L., L. Wilson, and B. I. Kiefer. 1978. Mitotic mechanism based on intrinsic microtubule behavior. *Nature (Lond.).* 272:450–452.
25. McIntosh, J. R., P. K. Hepler, and D. G. vanWie. 1969. Model for mitosis. *Nature (Lond.).* 224:659–663.
26. Meeusen, R., and W. Z. Cande. 1979. *N*-ethylmaleimide-modified heavy meromyosin: a probe for actomyosin interactions. *J. Cell. Biol.* 82:57–65.
27. Meeusen, R. L., J. Bennett, and W. Z. Cande. 1980. Effect of microinjected *N*-ethylmaleimide-modified heavy meromyosin on cell division in amphibian eggs. *J. Cell. Biol.* 86: 858–865.
28. Miller, M. R., J. J. Castellot, Jr., and A. B. Pardee. 1979. A general method for permeabilizing monolayer and suspension cultured animals cells. *Exp. Cell Res.* 120:421–425.
29. Nicklas, R. B. 1971. Mitosis. *In* Advances in Cell Biology. D. M. Prescott, L. Goldstein, and E. McConkey, editors. Appleton-Century-Crofts, New York. 2:225–297.
30. Nicklas, R. B. 1975. Chromosome movement: current models and experiments on living cells. *In* Molecules and Cell Movement. Inoué, S. and R. Stephens, editors. Raven Press, New York. 97–117.
31. Petzelt, C. 1979. Biochemistry of the mitotic spindle. *Int. Rev. Cytol.* 60:53–92.
32. Sakai, H., I. Mabuchi, S. Shimoda, R. Kuriyama, K. Ogawa, and H. Mohri. 1976. Induction of chromosome motion in the glycerol isolated mitotic apparatus: nucleotide specificity and effects of antidynein and myosin sera on the motion. *Dev. Growth Differ.* 18:211–219.
33. Salmon, E. D., and R. R. Segall. 1979. μM Ca^{+2} induces microtubule depolymerization and spindle fiber shortening in isolated mitotic cytoskeletons. *J. Cell. Biol.* 83 (2, Pt. 2): 337*a* (Abstr.).
34. Sanger, J. W. 1975. Presence of actin during chromosomal movement. *Proc. Natl. Acad. Sci. U. S. A.* 72:2451–2455.
35. Sanger, J. W. 1977. Mitosis in beating cardiac myoblasts treated with cytochalasin B. *J. Exp. Zool.* 201:463–469.
36. Schiff, P. B., and S. B. Horwitz. 1980. Taxol stabilizes microtubules in mouse fibroblast cells. *Proc. Natl. Acad. Sci. U. S. A.* 77:1561–1565.
37. Schloss, J. W., A. Milsted, and R. D. Goldman. 1977. Myosin subfragment-1 binding for the localization of actinlike microfilaments in cultured cells. A light and electron microscopy study. *J. Cell. Biol.* 74:794–815.
38. Schroeder, T. E. 1975. Dynamics of the contractile ring. *In* Molecules and Cell Movements. S. Inoué and R. E. Stephens, editors. Raven Press, New York. 305–332.
39. Snyder, J. A., and J. R. McIntosh. 1975. Initiation and growth of microtubules from mitotic centers in lysed mammalian cells. *J. Cell. Biol.* 67:744–760.
40. Tanenbaum, S. W. 1978. Cytochalasins. Biochemical and cell biological aspects. Elsevier/North Holland Biomedical Press, Amsterdam. 1–564.
41. Wang, Y., and D. L. Taylor. 1979. Distribution of fluorescently labeled actin in living sea urchin eggs during early development. *J. Cell. Biol.* 82:672–679.
42. Weeds, A., and R. Taylor. 1975. Separation of subfragment-1 isoenzymes from rabbit skeletal muscle myosin. *Nature (Lond.).* 257:54–56.
43. Wehland, J., M. Osborn, and K. Weber. 1977. Phalloidin induced actin polymerization in the cytoplasm of cultured cells interferes with cell locomotion and growth. *Proc. Natl. Acad. Sci. U. S. A.* 74:5613–5617.
44. Weingarten, M. D., A. H. Lockwood, S-Y. Hwo, and M. W. Kirschner. 1975. A protein factor essential for microtubule assembly. *Proc. Natl. Acad. Sci. U. S. A.* 72:1855–1862.